RSC Advances

PAPER

View Article Online
View Journal | View Issue

Cite this: *RSC Adv.*, 2019, **9**, 22240

Improving the anticancer activity of platinum(IV) prodrugs using a dual-targeting strategy with a dichloroacetate axial ligand†

Fengfan Liu,[a] Xiaomei Dong,[a] Qiwen Shi,[a] Jianli Chen[a] and Weike Su *[ab]

Four novel platinum(IV) complexes, characteristic of DCA/TFA and with chloride ions as axial ligands, were designed and synthesized. This type of platinum(IV) complexes **1a–2b** exhibited significant cytotoxic activity, and the cytotoxicity of **1b** was the greatest among these four complexes, which was 20.61 fold and 7.65 fold higher than that of cisplatin against HepG-2 and NCI-H460 cancer cells, respectively. The result from the apoptosis assay of **1b** was consistent with the result from the cytotoxicity assay. In addition, complexes **1a** and **1b** induced cell cycle arrest at the S phase on HepG-2 cells. Taken together, our data showed that Pt(IV) complex **1b** released the corresponding Pt(II) complex and DCA, and induced apoptosis as well as disruption of the mitochondrial membrane potential, establishing Pt(IV) complex **1b** as a potential dual-targeting anticancer agent.

Received 16th May 2019
Accepted 5th July 2019

DOI: 10.1039/c9ra03690c

rsc.li/rsc-advances

1. Introduction

The United States Food and Drug Administration (FDA) has approved cisplatin, carboplatin, and oxaliplatin for the treatment of cancer.[1,2] According to previous reports, platinum drugs were administered to 50–70% of cancer patients, either as single drugs or in combination with other drugs.[3] However, side effects and drug resistance have greatly limited the therapeutic application of platinum drugs.[3–6] Therefore, a variety of functional platinum complexes with different strategies have been studied to improve cancer therapy, including receptor targeting of platinum complexes, nano-delivery of platinum complexes and dual-threat platinum prodrugs.[7–12] In addition, the FDA has approved an immunotherapy for patients with a specific type of lung cancer in 2018, which needs adjuvant treatment with platinum-containing chemotherapy.[13,14] Therefore, through a process of continuous design for improvement, these drugs will still play an important role in the future.[15–18] In our previous research, complexes **A** and **B** exhibited similar activity compared with cisplatin and oxaliplatin, but their toxicity against normal cells was lower than that of cisplatin and oxaliplatin.[19,20] The results indicated that both of them were promising anticancer lead compounds for further study (Fig. 1).

Dichloroacetate (DCA), an enzyme pyruvate dehydrogenase kinase inhibitor, can reverse the Warburg effect by improving the way pyruvate enters mitochondria.[21] It can reduce tumor cell proliferation and promote cancer cell death *via* inducing apoptosis and mitochondrial dysfunction. In fact, Pt(II)/(IV) complexes could effectively increase the anticancer activity by introducing one or two DCA into the axial ligands (Fig. 1).[22–24] On the other hand, taking the trifluoroacetate (TFA) group as the ligand can increase the lipophilicity and possess good ability to be dissociated.[25,26] Therefore, we designed and synthesized Pt(IV) complexes **2a** and **2b** with TFA as the axial ligand.

Since platinum(IV) prodrugs have kinetic inertia and contain functional groups in the axial position, their characteristics include minimizing unwanted side reactions with biomolecules prior to activation of Pt(IV) prodrugs, enhancing the cytotoxicity of platinum complexes, regulating the reduction rate and altering the lipophilicity of resulting complexes. The bioactive molecule can ultimately combine with platinum(II) complex

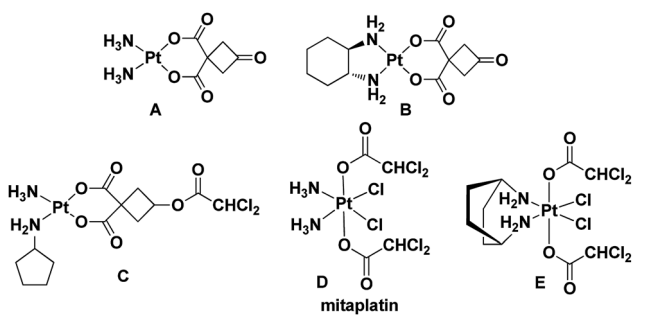

Fig. 1 Leading compounds (A and B) and known platinum complexes of ligands with dichloroacetate (C–E).

[a]*National Engineering Research Center for Process Decelopment of Active Pharmaceutial Ingredients, Collaborative Innovation Center of Yangtze River Delta Region Green Pharmaceuticals, Zhejiang University of Technology, Hangzhou, P. R. China. E-mail: pharmlab@zjut.edu.cn*

[b]*College of Pharmaceutical Sciences, Zhejiang University of Technology, Hangzhou, P. R. China*

† Electronic supplementary information (ESI) available. See DOI: 10.1039/c9ra03690c

dissociated from the platinum(IV) prodrug under the reductive condition to improve anti-tumor effects. Until now, cisplatin-based and oxaliplatin-based Pt(IV) complexes have been used to act as leading compounds. Herein, we designed and synthesized four novel Pt(IV) complexes **1a–2b** with a new structure to reduce side effects prior to activation of Pt(IV) prodrugs and target nuclear DNA and mitochondria (Scheme 1). This work was motivated idea from Mitaplatin analogue, which firstly displayed a dual-targeting strategy with dichloroacetate axial ligand.[22]

2. Results and discussion

2.1 Chemistry

Notably, Pt(IV) complexes **1a–2b** were synthesized by the oxidative chlorination of the corresponding platinum(II) complexes **A** and **B** with *N*-chlorosuccinimide in the acetone solution of dichloroacetic acid or trifluoroacetic acid, respectively. This procedure obtained Pt(IV) complexes adopting a one-pot synthesis (Scheme 1). All complexes were characterized by using IR, ^{1}H NMR, ^{13}C NMR and ESI-MS and elemental analysis. N–H stretching vibrations were found in the IR spectra of the platinum complexes ranging from 3061–3574 cm^{-1}. The coordination of the amino group to platinum(II) caused the difference between the vibrations. The presence of stretches between 2936 and 2939 cm^{-1} confirmed the presence of C–H bonds. In the ^{1}H NMR spectra, the cyclobutyl proton of complexes **A** and **B** appeared at a single peak in 3.71 ppm. These signals were completely different from those of the corresponding platinum(IV) complexes **1a–2b** appearing the split by the introduction ligands into the axial position. The $CHCl_2$ signal of the complexes **1a** and **1b** appeared at a single peak in 6.52 ppm and 6.49 ppm, respectively. In the ^{13}C NMR spectrum, the peaks at δ 67.1, 67.7 assignable to $CHCl_2$ carbon, at δ(62.4, 58.6), δ(62.6, 58.3) for C–N carbons (**1b** and **2b**), respectively. The ESI-MS showed $[M + Na]^+$ peaks that were in agreement with the proposed molecular formulas of the metal complexes.

2.2 Stability of complexes 1a–2b in PBS

The stability of complexes **1a** and **1b** in a solution of deuterated aqueous and phosphate buffered solution (PBS 7.87 mM, pH 7.4 in DMSO-d_6/D_2O ratio of 10 : 90 (v/v)) at 37 °C was investigated by ^{1}H NMR technique at different time. As shown in Fig. 2, the peak of coordinated DCA in complex **1a** located at 6.18 ppm. After 50 minutes incubation under the physiological condition, we observed the decay of the $CHCl_2$ signal at 6.18 ppm (marked with ▲ in Fig. 2) and the concomitant increase of a signal resonating at 5.86 ppm (● indicates the peak of free DCA). The half-life of **1a** was approximately 50 minutes, which had a value quite similar to that reported for kiteplatin (60 min).[20] Meanwhile, **1b** (60 min) has the same half-life as **1a** and kiteplatin in the same experimental conditions. As shown in Fig. S32 and S33,† the half-lives of complexes **1a** and **1b** were similar to those obtained by ^{1}H NMR. On the other hand, the characteristic peaks of complexes **2a** and **2b** are not so obvious in ^{1}H NMR. The stability of **2a** and **2b** in the solution of MeOH/PBS (v/v = 1 : 9) was examined by HPLC at different times. As shown in Fig. S34 and S35† (ESI†), the half-life of **2a** and **2b** was approximately 50–60 minutes under the physiological condition, which were lower than that found for *ct*-[$Pt(NH_3)_2$(TFA)$_2$(CBCDA)] (**5**) with TFA as axial ligands (PBS, 37 °C, pH 7.0, $t_{1/2}$ = 142 min).[27] Furthermore, the complexes **1a–2b** were stable in methanol for 48 hours (S36–S39†).

2.3 *In vitro* cytotoxicity assay

The cytotoxicity of complexes **1a–2b** was first tested *in vitro* by MTT assay in BGC803, HepG-2, MCF-7 and NCI-H460 cancer cell lines with cisplatin, oxaliplatin, and carboplatin as positive controls. The IC_{50} values of them were reported in Table 1.

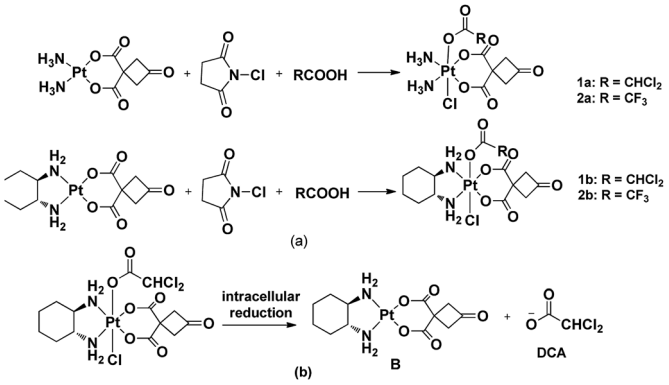

Scheme 1 (a) Synthetic route of target complexes **1a–2b**; (b) proposed mechanism of activation of **1b**.

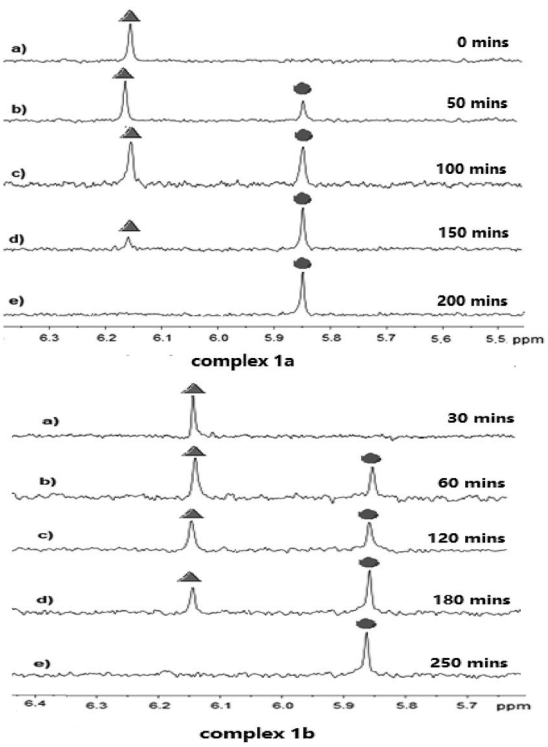

Fig. 2 Portion of the ^{1}H NMR (400 MHz) spectra of complexes **1a** and **1b** in deuterated aqueous and phosphate buffered solution (PBS 7.87 mM, pH 7.4; at 37 °C; 10% v/v DMSO-d_6). ▲ indicates the peak of coordinated DCA in complex **1a** and **1b**. ● indicates the peak of free DCA.

Table 1 *In vitro* cytotoxicity of complexes **1a–2b**, cisplatin, carboplatin and oxaliplatin

	IC_{50}[a] (μM)			
Complex	BGC803[b]	HepG-2[c]	MCF-7[d]	NCI-H460[e]
Cisplatin	21.58 ± 1.35	27.82 ± 2.56	29.19 ± 1.38	14.85 ± 1.35
Oxaliplatin	29.10 ± 1.65	26.49 ± 2.55	41.27 ± 3.43	13.43 ± 1.13
Carboplatin	77.14 ± 5.35	42.32 ± 2.55	179.40 ± 10.56	52.93 ± 4.98
DCA	>100	>100	>100	>100
A : DCA (1 : 1)	431.11 ± 15.56	99.47 ± 2.89	11.36 ± 1.56	10.22 ± 0.99
B : DCA (1 : 1)	190.06 ± 13.51	41.09 ± 3.02	60.46 ± 4.85	18.86 ± 1.19
1a	57.73 ± 4.34	10.36 ± 1.24	27.08 ± 2.25	>200
1b	7.63 ± 0.56	1.35 ± 0.15	7.96 ± 0.76	1.94 ± 0.13
2a	14.09 ± 0.98	15.00 ± 1.42	22.63 ± 2.05	5.46 ± 0.43
2b	15.01 ± 1.05	17.54 ± 1.65	22.20 ± 2.17	7.66 ± 0.57

[a] IC_{50} is the drug concentration effective in inhibiting 50% of the cell growth measured by the MTT assay after 48 h drug exposure. [b] BGC803: human gastric cancer cell line. [c] HepG-2: human hepatocellular carcinoma cell line. [d] MCF-7: human breast carcinoma cell line. [e] NCI-H460: large cell lung cancer cell line.

These four complexes displayed potent antitumor activity against BGC803, HepG-2, MCF7 and NCI-H460 cancer cell lines with the IC_{50} values in the range of 7.63–57.73 μM, 1.35–17.54 μM, 7.96–27.08 μM and 1.94–200 μM, respectively. Among them, complex **1b** showed the highest activity against four cancer cell lines, which was superior to positive controls (cisplatin, oxaliplatin and carboplatin). DCA had no obvious cytotoxic activity on cancer cell lines with the IC_{50} values exceeding 100 μM. It was noted that **1b** exhibited higher cytotoxic activity than an equivalent mixture: DCA : **A** (1 : 1) and DCA : **B** (1 : 1), implying that the special structure of complex **1b** resulted in better cytotoxic activity. Notably, complex **1b** exhibited 20.61 fold and 7.65 fold higher cytotoxicity toward HepG-2 and NCI-H460 cancer cells than that of cisplatin. Meanwhile, the cytotoxic activity of complex **1b** was 2.82 fold and 3.66 fold more potent than that of cisplatin against BGC803 and MCF-7, respectively.

By the analysis of the structure–activity relationship and cytotoxic activity, the design of novel Pt(IV) **1a** and **1b** effectively improved the anti-tumor activity. Moreover, taking this type of complexes as prodrugs could reduce the attack of small sulfur-containing molecules (*e.g.*, glutathione, methionine and metallothionein) and maintain a relatively stable structure before reaching tumor cells. After that, complexes **1a** and **1b** could release **B** and DCA, playing a dual-targeting anti-tumor effect against cancer cells, targeting nuclear DNA and mitochondria, respectively. In addition, complexes **2a** and **2b** exhibited good effects against BGC803, HepG-2, MCF-7 and NCI-H460 cancer cell lines, demonstrating that the axial ligand can be modified to alter the reductive rate and the lipophilicity of Pt(IV) complexes and consequently enhance the anti-tumor activity of Pt(IV) complexes.

Based on the above results, complexes **1a–2b** were selected for further investigation against SGC7901, SGC7901/CDDP and HUVEC cells lines by MTT assay. As shown in Table 2, complexes **1a** and **1b** showed the same cytotoxicity as oxaliplatin against SGC7901. However, SGC7901/CDDP cell line was not sensitive to all the tested compounds, indicating that these compounds were not able to overcome cisplatin resistance. In HUVEC, the cytotoxicity of complexes **1a** and **1b** (IC_{50} = 59.11 μM and IC_{50} = 56.92 μM) was lower than that of cisplatin (IC_{50} = 36.92 μM). Meanwhile, neither compounds **2a** nor **2b** had detectable cytotoxic activity on HUVEC with IC_{50} values exceeding 200 μM. This type of Pt(IV) complexes was more selective to tumor cells compared with HUVEC. Consequently, both complexes **1a** and **1b** were promising anticancer candidates for further research.

2.4 Cellular uptake

Given that complexes **1a** and **1b** exhibited better cytotoxicity, they were chosen to conduct a cellular uptake test on HepG-2 and NCI-H460 cells by using ICP-MS. As for HepG-2 cell line, platinum accumulation of **1b** was 1.28 times more potent than that of cisplatin. Meanwhile, the intracellular Pt levels of **1a** and **1b** were higher than that of cisplatin due to the lipophilicity, while complex **1a** had the same Pt content as **1b** in HepG-2 cells. Interestingly, the uptake of complex **1b** by NCI-H460 cells was 2.32 times higher than that of **1a**.

According to Tables 1 and 3, it seems that enhanced cellular uptake is associated with increased cytotoxicity of complexes. However, the intracellular platinum level is not the only factor

Table 2 *In vitro* cytotoxicity of complexes **1a–2b**, cisplatin and oxaliplatin

	IC_{50}[a] (μM)		
Complex	SGC7901[b]	SGC7901/CDDP[c]	HUVEC[d]
Cisplatin	9.96 ± 0.87	35.65 ± 2.55	36.92 ± 2.23
Oxaliplatin	13.47 ± 1.55	99.44 ± 5.23	51.03 ± 4.42
1a	16.79 ± 1.45	92.45 ± 2.56	59.11 ± 2.54
1b	16.76 ± 1.78	120.16 ± 6.74	56.47 ± 1.65
2a	20.15 ± 1.44	92.65 ± 1.56	>200
2b	8.73 ± 1.87	97.50 ± 3.67	>200

[a] IC_{50} is the drug concentration effective in inhibiting 50% of the cell growth measured by the MTT assay after 48 h drug exposure. [b] SGC7901: gastric cancer cell line. [c] SGC7901/CDDP: cisplatin-resistant gastric cancer cell line. [d] HUVEC: human umbilical vein endothelial cell line.

Table 3 Cellular uptake of **1a** and **1b** in HepG-2 and NCI-H460 cells after 12 h of incubation[a]

	Pt content[b] (nanograms per 10^6 cells)	
Complex	HepG-2	NCI-H460
Cisplatin	176 ± 15	189 ± 20
Oxaliplatin	188 ± 12	196 ± 19
1a	213 ± 17	106 ± 17
1b	227 ± 26	246 ± 31

[a] HepG-2 and HCI-H460 cells were treated with 20 μM of cisplatin, oxaliplatin, complexes **1a** and **1b** for 12 h. [b] Results are expressed as the mean ± SD for four independent experiments.

deciding the cytotoxicity of platinum complexes. In fact, many other factors also affect the cytotoxic activity of platinum complexes, such as the effective amounts of the compounds that finally act on DNA. Actually, we have already found similar results in previous studies.[28–30]

2.5 Complex 1a and 1b induced apoptotic cell death

Since complexes **1a** and **1b** showed better cytotoxicity, they were selected to carry out the apoptotic study against HepG-2 cells by Annexin V-FITC/PI assay. HepG-2 cells were incubated with 50 μM of indicated complexes for 24 hours. The quadrants Q1–Q4 represented four different cancer cell states: necrotic cells, late apoptotic or necrotic cells, living cells and early apoptotic cells, respectively.

Table 4 Red-green fluorescence ratio of positive controls and target complexes **1a** and **1b**[a]

Complex	Ratio (FL2/FL1)
Negative control	5.42
CCCP	0.04
DCA	4.17
Cisplatin	0.54
Carboplatin	2.56
Oxaliplatin	0.94
1a : DCA (1 : 1)	0.59
1b : DCA (1 : 1)	0.80
1a	0.98
1b	0.86

[a] HepG-2 cells cultured in the presence of 30 μM of cisplatin, carboplatin, oxaliplatin, complex **1a** or **1b** for 48 hours at 37 °C (DMF final concentration < 0.4%). Then the cells were harvested by centrifugation and incubated with JC-1 solution for 30 min. After briefly washing, the proportions of red and green fluorescence intensity were immediately detected and analyzed by flow cytometry (Ex = 488 nm; Em = 530 nm).

As shown in Fig. 3, complexes **1a** and **1b** (28.75% and 28.97%) had nearly the same apoptotic rate as cisplatin (28.79%) against HepG-2 cells while showing a higher apoptotic rate than oxaliplatin (21.74%; Fig. 2). As for HepG-2 cell line, after treated with **1b** for 24 hours, the early apoptotic rate rose strikingly from 2.14% to 24.97% and the late apoptotic rate was increased from 4.17% to 4.99%. Similarly, the early apoptotic rate of HepG-2 cell for **1a** surged from 2.14% to 21.61% and the

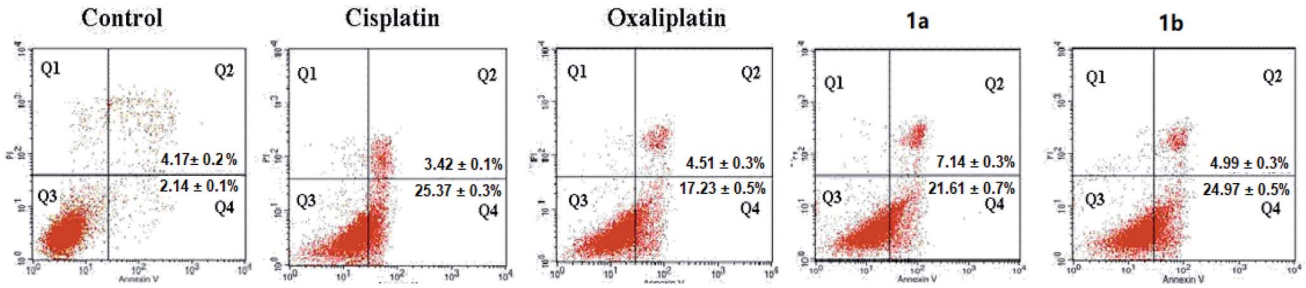

Fig. 3 Flow cytometric analysis of the distribution of HepG-2 cells treated with 50 μM of cisplatin, oxaliplatin, complexes **1a** and **1b** for 24 hours (DMF final concentration < 0.4%). Cells were stained with 5 mL of Annexin V-FITC and incubated in the dark at 25 °C for 10 min. The fluorescence was measured by using a flow cytometer. The results were expressed as the percentage of normal and apoptotic cells at various stages by FCS Express software.

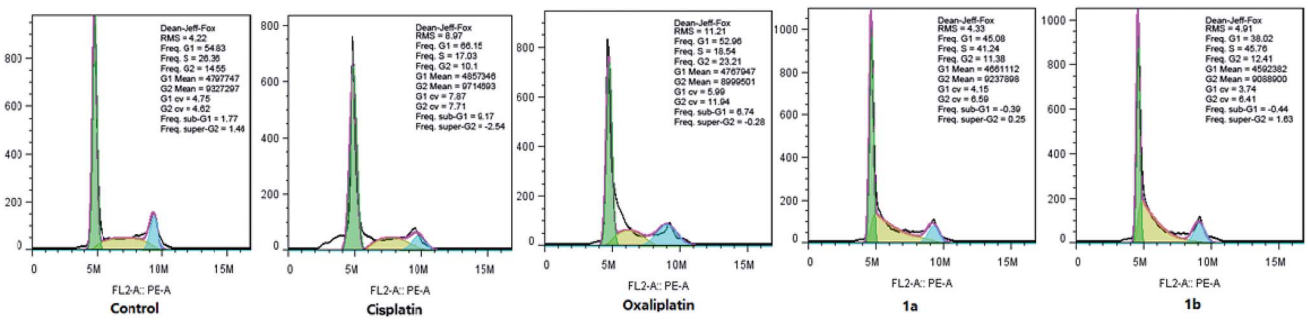

Fig. 4 Cell cycle distribution of HepG-2 cells cultured in the presence of 30 μM of cisplatin, oxaliplatin, complexes **1a** and **1b** (DMF final concentration < 0.4%). The cells were seeded in 6-well plates for 12 hours at 37 °C, and then were treated with cisplatin, oxaliplatin, complex **1a** or **1b**. After 12 hours of treatment, cells were harvested with trypsin and washed twice with PBS.

Table 5 Molecular formulas and $[M + Na]^+$ experimental and theoretical of **1a–2b**

	Molecular formula	$[M + Na]^+$ experimental	$[M + Na]^+$ theoretical	Error [ppm]
1a	$C_8H_{11}Cl_3N_2O_7Pt$	569.9196	569.9172	−4.0
1b	$C_{14}H_{19}Cl_3N_2O_7Pt$	649.9818	649.9798	−2.9
2a	$C_8H_{10}ClF_3N_2O_7Pt$	555.9687	555.9669	−3.2
2b	$C_{14}H_{18}ClF_3N_2O_7Pt$	636.0323	636.0295	−4.2

late apoptotic rate was increased from 4.17% to 7.14%. Complex **1b** showed a slightly higher population of apoptotic cells than complex **1a** did. Based on the results from the cytotoxicity tests and the apoptotic assays, it was noted that there might be a positive correlation between these two assays. The order of apoptotic rates against HepG-2 cells from high to low was **1b**, **1a**, cisplatin, and oxaliplatin. Complexes **1a** and **1b** were able to cause cancer cell death through apoptotic pathways.

2.6 Effect on cell cycle arrest

It is confirmed that cell cycle contains four different phases, including G1, G2, S, and M stages. Pt(IV) complexes could inhibit cancer cell growth by cell cycle arrest. As shown in Fig. 4, HepG-2 cells were treated with cisplatin, oxaliplatin, complex **1a** or **1b** for 12 hours, and the cell cycle distribution was examined by PI staining and following flow cytometry analysis.

The percentage of cells at G1 phase was increased significantly upon cisplatin treatment (from 54.83% to 66.15%), while oxaliplatin arrested HepG-2 cells at G2 phase (from 14.55% to 23.21%). Notably, the cell cycle arrest caused by complex **1a** and **1b** mainly occurred at S phase (from 26.36% to 41.24% and from 26.36% to 45.76%). Overall, it was confirmed that different from cisplatin and oxaliplatin, complex **1a** and **1b** induced cell cycle arrest at S phase by inhibiting DNA replication in the nucleus. The different feature of cell cycle arrest is probably due to distinct DNA binding modes.

2.7 Mitochondrial membrane potential

Platinum(IV) complexes **1a** and **1b** can release platinum(II) complexes and DCA under the intracellular reductive condition, targeting nuclear DNA and mitochondria, respectively. In addition, DCA can result in mitochondrial dysfunction, and the change of mitochondrial function is manifested as the decrease in membrane potential and stability. The change of transmembrane potential causes the release of cytochrome C and a variety of apoptosis inducing factors (AIFs), which activate a cascade of apoptosis and eventually lead to apoptosis. In order to confirm that the change of mitochondria membrane potential was caused by Pt(IV) complexes, HepG-2 cells were incubated with the tested complexes for 48 hours and examined by JC-1 staining method.

Complexes **1a** and **1b** were selected to test their effects on mitochondrial membrane potential with carbonylcyanide-*m*-chlorophenylhydrazone (CCCP), DCA, cisplatin, carboplatin and oxaliplatin as positive controls. As shown in Table 4, compared with the negative control, red-green fluorescence ratio of each group was dropped. In fact, complexes **1a** and **1b** notably reduced the mitochondrial membrane potential (FL2/FL1 = 0.98 and FL2/FL1 = 0.86). However, the decrease caused by complexes **1a** and **1b** was less than that induced by **1a** : DCA (1 : 1) and **1b** : DCA (1 : 1) (FL2/FL1 = 0.59 and FL2/FL1 = 0.80). The decline of mitochondrial membrane potential was a landmark event in the early stage of apoptosis, and the IC_{50} values of complexes **1a** and **1b** were lower than an equivalent mixture: DCA : **A** (1 : 1) and DCA : **B** (1 : 1). Besides, complexes **1a** and **1b** could release the corresponding platinum(II) and DCA by reduction, which could target mitochondria.

3. Conclusions

In this manuscript, we explored two types of Pt(IV) complexes **1a–1b** and **2a–2b** by taking complexes **A** and **B** as the lead compounds, and investigated dual-threat platinum prodrugs and the lipophilicity of the TFA as the axial ligand, respectively. Complexes **1a** and **1b** could rapidly transform in PBS (pH = 7.4) with the hydrolysis of the axial DCA ligands ($t_{1/2}$ = 60 min). According to the IC_{50} values, **1a** and **1b** had better cytotoxic activity than cisplatin, oxaliplatin and carboplatin against HepG-2 and MCF-7 cell lines. Since Pt(IV) prodrugs **1a–2b** had relatively kinetic inertia, they possessed less toxicity than cisplatin and oxaliplatin against HUVEC cell line. In addition, it was confirmed that complexes **1a** and **1b** induced cell cycle arrest at S phase (41.24% and 45.76%) by inhibiting DNA replication in the nucleus. Moreover, both of them significantly reduced the mitochondrial membrane potential. Above all, platinum(IV) prodrugs could improve the anticancer activity using a dual-targeting strategy with dichloroacetate axial ligand, which released platinum(II) complexes and DCA under the intracellular reductive condition, targeting nuclear DNA and mitochondria, respectively.

Furthermore, a series of novel platinum complexes with ethylenediamine-*N*,*N*′-di-2/3-propionate ester as ligands has been reported to induce caspase-dependent apoptosis.[31] Therefore, it is still a reasonable way to design antitumor platinum complexes targeting nuclear DNA and mitochondria. It may be an interesting approach to combine such complexes with drug delivery systems in the future.

4. Experimental

4.1 Chemistry

Materials and methods. All reagents and solvents were of analytical grade and were used without further purification. Complexes **A** and **B** were prepared as described in our previous

study.[19] All tumor cell lines were purchased from Hangzhou Hibio bioTech company. ^{1}H NMR and ^{13}C NMR spectra were recorded in DMSO-d_6 on a Bruker 300 MHz or 500 MHz spectrometer. Platinum contents were determined by an inductively coupled plasma-mass spectrometer (ICP-MS, Optima 5300DV, PerkinElmer, USA). Mass spectra were measured on an Agilent 6224 ESI/TOF MS instrument.

Dichloroacetatodiamminechlorido(3-oxo-1,1-cyclobutanedicarboxylato)platinum(IV) (1a). Complex **A** (0.38 g, 1.00 mmol), dichloroacetic acid (3 mL) and acetone (50 mL) were added into a 100 mL reaction bottle. The acetone solution (10 mL) of *N*-chlorobutanedimide (0.14 g, 1.05 mmol) was then added into the reaction system slowly, which was reacted at 25 °C for 12 hours. Then the organic phase was evaporated under reduced pressure, obtaining the viscous light yellow compound **1a**. Furthermore, complex **1a** was precipitated out by adding diethyl ether (150 mL), which was washed with a small amount of ethanol several times and dried *in vacuo*. White solid, yield: 0.36 g (67%). IR (KBr, cm^{-1}): 3168m, 3064m, 2924m, 2870m, 1791m, 1625s, 1371m, 1025m; ^{1}H NMR (300 MHz, d_6-DMSO): δ 3.50 (s, 2H, CH_2 of cyclobutane), 3.57 (s, 2H, CH_2 of cyclobutane), 6.01–6.44 (m, 6H, 2× NH_3), 6.52 (s, 1H, $CHCl_2$); ^{13}C NMR (75 MHz, d_6-DMSO): 204.0, 176.1, 169.2, 67.1, 60.2, 59.8, 46.0; HR-MS (*m*/*z*) (ESI): calcd for $C_8H_{11}Cl_3N_2NaO_7Pt$ $[M + Na]^+$, 569.9172; found, 569.9196. Elemental analysis calcd (%) for $C_8H_{11}Cl_3N_2O_7Pt$: C, 17.51; H, 2.02; N, 5.11; found: C, 17.47; H, 2.14; N, 5.13.

Dichloroacetato(cyclohexane-1*R*,2*R*-diamine)chlorido(3-oxo-1,1-cyclobutanedicarboxylato)platinum(IV) (1b). Complex **B** (0.47 g, 1.00 mmol), dichloroacetic acid (3 mL) and acetone (50 mL) were added into a 100 mL reaction bottle. The acetone solution (10 mL) of *N*-chlorobutanedimide (0.14 g, 1.05 mmol) was then added into the reaction system slowly, which was reaction reacted at 25 °C for 18 hours. After the reaction, organic phase was evaporated under reduced pressure, obtaining the viscous light yellow compound **1b**. Furthermore, complex **1b** was precipitated out by adding diethyl ether (150 mL). Complex **1b** was washed with a small amount of ethanol several times and dried *in vacuo*. White solid, yield: 0.27 g (52%). IR (KBr, cm^{-1}): 3170m, 3061m, 2936m, 2872m, 1793m, 1626s, 1370m, 1027m; ^{1}H NMR (300 MHz, d_6-DMSO): δ 1.00–1.14 (m, 2H, CH_2 of DACH), 1.38–1.57 (m, 4H, 2× CH_2 of DACH), 1.97–2.09 (m, 2H, CH_2 of DACH), 2.58–2.66 (m, 2H, 2× $CHNH_2$), 3.14 (m, 2H, CH_2 of cyclobutane), 3.61 (s, 2H, CH_2 of cyclobutane), 6.49 (s, 1H, $CHCl_2$), 7.51–8.26 (m, 4H, 2× NH_2); ^{13}C NMR (75 MHz, d_6-DMSO): 203.6, 176.6, 168.4, 67.7, 62.4, 61.4, 61.1, 58.6, 46.4, 31.3, 30.8, 24.0, 23.9; HR-MS (*m*/*z*) (ESI): calcd for $C_{14}H_{19}Cl_3N_2NaO_7Pt$ $[M + Na]^+$, 649.9798; found, 649.9818; elemental analysis calcd (%) for $C_{14}H_{19}Cl_3N_2O_7Pt$: C, 26.74; H, 3.05; N, 4.46; found: C, 26.83; H, 3.11; N, 4.38.

Trifluoroacetatodiamminechlorido(3-oxo-1,1-cyclobutanedicarboxy-lato)platinum(IV) (2a). Complex **A** (0.38 g, 1.00 mmol), trifluoroacetic acid (3 mL) and acetone (50 mL) were added into a 100 mL reaction bottle. The acetone solution (10 mL) of *N*-chlorobutanedimide (0.14 g, 1.05 mmol) was then added into the reaction system slowly, which was reaction reacted at 25 °C for 12 hours. After the reaction, organic phase was evaporated under reduced pressure, obtaining the viscous light yellow compound **2a**. Furthermore, complex **2a** was precipitated out by adding diethyl ether (150 mL). Complex **2a** was washed with a small amount of ethanol several times and dried *in vacuo*. White solid, yield: 0.39 g (63%). IR (KBr, cm^{-1}): 3574m, 3247m, 3103m, 1783m, 1668m, 1360m, 1207m, 1123m; ^{1}H NMR (300 MHz, d_6-DMSO): δ 3.48 (s, 2H, CH_2 of cyclobutane), 3.51 (s, 2H, CH_2 of cyclobutane), 6.20–6.58 (m, 6H, 2× NH_3); ^{13}C NMR (75 MHz, d_6-DMSO): 203.3, 176.1, 166.3, 60.0, 59.8, 46.1; HR-MS (*m*/*z*) (ESI): calcd for $C_8H_{10}ClF_3N_2NaO_7Pt$ $[M + Na]^+$, 555.9669; found, 555.9687; elemental analysis calcd (%) for $C_8H_{10}ClF_3N_2O_7Pt$: C, 18.00; H, 1.89; N, 5.25; found: C, 18.06; H, 1.84; N, 5.27.

Trifluoroacetato(cyclohexane-1*R*,2*R*-diamine)chlorido(3-oxo-1,1-cyclobutanedicarboxylato)platinum(IV) (2b). Complex **B** (0.47 g, 1.00 mmol), trifluoroacetic acid (3 mL) and acetone (50 mL) were added into a 100 mL reaction bottle. The acetone solution (10 mL) of *N*-chlorobutanedimide (0.14 g, 1.05 mmol) was then added into the reaction system slowly, which was reaction reacted at 25 °C for 18 hours. After the reaction, organic phase was evaporated under reduced pressure, obtaining the viscous light yellow compound **2b**. Furthermore, complex **2b** was precipitated out by adding diethyl ether (150 mL). Complex **2b** was washed with a small amount of ethanol several times and dried *in vacuo*. White solid, yield: 0.35 g (57%). IR (KBr, cm^{-1}): 3561m, 3468m, 2939m, 1796m, 1719m, 1633m, 1370m, 1178m; ^{1}H NMR (300 MHz, d_6-DMSO): δ 0.99–1.13 (m, 2H, CH_2 of DACH), 1.48–1.52 (m, 4H, CH_2 of DACH), 1.96–2.08 (m, 2H, CH_2 of DACH), 2.60–2.62 (m, 2H, 2× $CHNH_2$), 3.29 (s, 2H, CH_2 of cyclobutane), 3.63 (s, 2H, CH_2 of cyclobutane), 7.63–8.37 (m, 4H, 2× NH_2); ^{13}C NMR (75 MHz, d_6-DMSO): 203.6, 176.7, 176.6, 62.6, 61.3, 61.2, 58.3, 46.5, 31.1, 30.7, 24.0, 23.9; HR-MS (*m*/*z*) (ESI): calcd for $C_{14}H_{18}ClF_3N_2NaO_7Pt$ $[M + Na]^+$, 636.0295; found, 636.0323; elemental analysis calcd (%) for $C_{14}H_{18}ClF_3N_2O_7Pt$: C, 27.39; H, 2.96; N, 4.56; found: C, 27.36; H, 2.84; N, 4.63 (Table 5).

Stability of 1a–2b in PBS. The solution behavior of **1a** and **1b** were investigated by ^{1}H NMR spectroscopy. Complexes **1a** and **1b** (0.786 μmol) was dissolved in DMSO-d_6 (0.5 mL). 100 μL of the previous solution was diluted with 900 μL of a deuterated aqueous phosphate buffered solution (PBS 7.87 mM, pH 7.4; at 37 °C) obtaining a final solution (DMSO-d_6/D_2O, 10 : 90 (v/v)). ^{1}H NMR spectra recorded at different time intervals.

Complexes **2a** and **2b** (0.786 μmol) were dissolved in MeOH (1 mL). The stability of **2a** and **2b** in a MeOH/PBS (1 : 9) was investigated by HPLC (PBS 7.87 mM, pH 7.4; at 37 °C). HPLC recorded at different time intervals. Reversed phase HPLC was implemented on a 250 × 4.6 mm ODS column and the HPLC profiles were recorded on UV detection at 226 nm. Mobile phase consisted of MeCN : H_2O = 25 : 75 (v/v), and flow rate was 1.0 mL min^{-1}. The samples were taken for HPLC analysis after filtration by 0.5 μm filter.

4.2 Bioactivity study

Cell culture. All adherent cell lines, including human gastric cancer cell line (BGC803), human hepatocellular carcinoma cell line (HepG-2), human breast carcinoma cell line (MCF-7), large

cell lung cancer cell line NCI-H460, gastric cancer cell line (SGC7901), cisplatin-resistant gastric cancer cell line (SGC7901/CDDP), and human umbilical vein endothelial cell line (HUVEC) were cultured in a humidified, 5% CO_2 atmosphere at 37 °C and kept in monolayer culture in DMEM medium supplemented with 10% fetal bovine serum (FBS), 100 mg mL^{-1} of streptomycin and 100 mg mL^{-1} of penicillin. All cell lines used in this study were obtained form KeyGen biotech company.

MTT assay. The cells were seeded in 96-well tissue cultured plates at a density of 5×10^3 cells per well. After overnight incubation, the cells were treated with the diluted solution of complexes, which were obtained by dissolving in DMF and diluting with culture medium (DMF final concentration < 0.4%). After 48 hours of incubation at 37 °C, 10 μL of a freshly diluted 3-(4,5-dimethyl-2-thiazolyl)-2,5-diphenyl-2*H*-tetrazolium bromide (MTT) solution (5 mg mL^{-1}) were added to each well and the plate was incubated at 37 °C in a humidified 5% CO_2 atmosphere for 4 hours. At the end of the incubation period, the medium was removed and the formazan product was dissolved in 150 μL of DMSO. The cell viability was evaluated by measurement of the absorbance at 570 nm, using an absorbance reader (Bio-Rad). IC_{50} values were calculated from curves constructed by plotting cell survival inhibitory rate (%) *versus* drug concentration logarithm. The reading values were converted to the percentage of control (% cell survival). Finally, cytotoxic effects were expressed as IC_{50} values.

Cellular uptake test. HepG-2 and NCI-H460 cells were seeded in 6-well plates. After the cells reached about 80% confluence, 20 μM of cisplatin, oxaliplatin, **1a** and **1b** were added, respectively. After 12 hours incubation, cells were collected and washed 3 times with ice-cold PBS then centrifuged at 1000 g for 10 min and resuspended in 1 mL of PBS. A volume of 100 μL was taken out to determine the cell density. The rest of the cells was spun down and digested at 65 °C in 200 μL of 65% HNO_3 for 10 hours. The content of Pt level in cells was obtained by ICP-MS.

Cell apoptosis study by flow cytometry. Apoptosis induced by platinum complexes was tested by flow cytometry using an Annexin V-FITC apoptosis detection kit according to the manufacturer's instructions. Flow cytometric analysis of the distribution of HepG-2 cells treated with cisplatin, oxaliplatin, complex **1a** and **1b** at 50 μM for 24 hours, and cells were collected by centrifugation (5 min, 25 °C, 2000 rpm). The cells were then washed twice with cold water and resuspended in Annexin V-FITC binding buffer (0.1 M Hepes/NaOH (pH 7.4), 1.4 M NaCl, 25 mM $CaCl_2$) at a concentration of 1×10^6 cells mL^{-1}. Cells were stained with 5 mL of Annexin V-FITC and incubated in the dark at 25 °C for 10 min. The cell suspension was centrifuged for 5 min (25 °C, 2000 rpm), and cells were resuspended in Annexin V-FITC binding buffer. Propidium iodide (10 mL) was added, and the tubes were placed on ice, away from light. The fluorescence was measured by using a flow cytometer (FACScan, Becton Dickson, USA). The results were expressed as the percentage of normal and apoptotic cells at various stages by FCS Express software.

Effect on cell cycle arrest. HepG-2 cells with a large amount of 1×10^6 were inoculated in 6-well plate and incubated at 37 °C in 5% CO_2 overnight. Cisplatin, oxaliplatin, complex **1a** and **1b** at the dose of 30 μM were treated with the cells for 12 hours respectively, and then cells were harvested with trypsin and washed twice with PBS. Moreover, cells were fixed in cold 70% ethanol and stored at 4 °C for 24 hours. After washing in PBS, cells were treated with RNase (75 kU mL^{-1}) for 30 min at 37 °C. Propidium iodide was finally added to stain cells and fluorescence intensity was monitored by a flow cytometer. Finally, 1×10^4 cells were acquired for each analysis.

Mitochondrial membrane potential. JC-1 (Beyotime, China), as a lipophilic cationic dye, was used to monitor the level of MMP in the cells. At normal state, the MMP is high and JC-1 appears as aggregates showing red fluorescence. However, when apoptosis occurs, the MMP reduced and JC-1 displayed as monomers, which is indicated by green fluorescence. In order to confirm that the change of mitochondria membrane potential was caused by the Pt(IV) complexes, the tested complexes were incubated with HepG-2 for 48 hours by JC-1 staining method. For flow cytometry analysis, HepG-2 cells were plated in 6-well plates (3×10^5 cells per well) and grown for 24 hours, and treated with complexes **1a** and **1b** at the indicated concentrations for 48 hours. Then the cells were harvested by centrifugation and incubated with JC-1 solution for 30 min. After briefly washing, the proportions of red and green fluorescence intensity were immediately detected and analysed by flow cytometry (Ex = 488 nm; Em = 530 nm).

Conflicts of interest

The authors declare no competing financial interest.

Acknowledgements

We are grateful to the China Postdoctoral Science Foundation (no. 2016M600473), the Postdoctoral Science Foundation of Zhejiang Province (no. zj20160107), and the National Natural Science Foundation of China (Project 21808205) for financial aids to this work. We are grateful to the Zhejiang Provincial Key R&D Project (No. 2018C03074). We thank the Jiangsu Province Hi-Tech Key Laboratory for Biomedical Research at Southeast University for completing the *in vitro* tests.

Notes and references

1 D. M. Cheff and M. D. Hall, *J. Med. Chem.*, 2017, **60**, 4517–4532.
2 N. J. Wheate, S. Walker, G. E. Craig and R. Oun, *Dalton Trans.*, 2010, **39**, 8113–8127.
3 J. D. White, M. F. Osborn, A. D. Moghaddam, L. E. Guzman, M. M. Haley and V. J. DeRose, *J. Am. Chem. Soc.*, 2013, **135**, 11680–11683.
4 R. A. Hazlitt, J. Min and J. Zuo, *J. Med. Chem.*, 2018, **61**, 5512–5524.
5 R. Qun, Y. E. Moussa and N. J. Wheate, *Dalton Trans.*, 2018, **47**, 6645–6653.
6 E. Martinez-Balibrea, A. Martinez-Cardus, A. Gines, V. R. Porras, C. Moutinbo, L. Layos, J. L. Manzano,

C. Buges, S. Bystrup, M. Esteller and A. Abad, *Mol. Cancer Ther.*, 2015, **14**, 1767–1776.

7 X. Y. Wang, X. H. Wang and Z. J. Guo, *Acc. Chem. Res.*, 2015, **48**, 2622–2631.

8 M. Yang, H. Z. Wu, J. L. Chu, L. A. Gabriel, K. S. Anderson, C. M. Furdui and U. Bierbach, *Chem. Commun.*, 2018, **54**, 7479–7482.

9 A. Abu Ammar, R. Raveendran, D. Gibson, T. Nassar and S. Benita, *J. Med. Chem.*, 2016, **59**, 9035–9046.

10 N. Wang, Z. G. Wang, Z. F. Xu, X. F. Chen and G. Y. Zhu, *Angew. Chem., Int. Ed.*, 2018, **57**, 3426–3430.

11 D. Y. Q. Wong, J. Y. Lau and W. H. Ang, *Dalton Trans.*, 2012, **41**, 6104–6111.

12 K. Mitra, C. E. Lyons and M. C. T. Hartman, *Angew. Chem., Int. Ed.*, 2018, **57**, 10263–10267.

13 G. De Lima Lopes, Y. L. Wu, S. Sadowski, J. Zhang, R. Rangwala, D. Kush and T. Mok, *J. Thorac. Oncol.*, 2016, **11**, S244–S245.

14 C. A. Garcia, S. Dacic and L. C. Villaruz, *J. Thorac. Oncol.*, 2018, **13**, e135–e136.

15 Z. Z. Zhu, Z. H. Wang, C. L. Zhang, Y. J. Wang, H. M. Zhang, Z. J. Gan and Z. J. Guo, *Chem. Sci.*, 2019, **10**, 3089–3095.

16 F. F. Chen, G. Xu, X. D. Qin, X. F. Jin and S. H. Gou, *J. Pharmacol. Exp. Ther.*, 2017, **263**, 221–239.

17 E. Gabano, M. Ravera, E. Perin, I. Zanellato, B. Rangone, M. J. McGlinchey and D. Osella, *Dalton Trans.*, 2019, **48**, 435–445.

18 X. Y. Yao, C. M. Tracy and U. Bierbach, *Inorg. Chem.*, 2019, **58**, 43–46.

19 J. Zhao, S. H. Gou and F. F. Liu, *Chem.–Eur. J.*, 2014, **20**, 15216–15225.

20 F. H. Chen, X. F. Jing, J. Zhao and S. H. Gou, *Exp. Cell Res.*, 2018, **364**, 68–83.

21 E. D. Michelakis, L. Webster and J. R. Mackey, *Cancer*, 2008, **99**, 989–994.

22 S. Dhar and S. J. Lippard, *Proc. Natl. Acad. Sci. U. S. A.*, 2009, **106**, 22199–22204.

23 W. P. Liu, J. Su, J. Jiang, X. Y. Li, Q. S. Ye, H. Y. Zhou, J. L. Chen and Y. Li, *Sci. Rep.*, 2013, **3**, 2464.

24 S. Savino, V. Gandin, J. D. Hoeschele, C. Marzano, G. Natile and N. Margiotta, *Dalton Trans.*, 2018, **47**, 7144–7158.

25 N. Margiotta, P. Papadia, F. Lazzaro, M. Crucianelli, F. De Angelis, C. Pisano, L. Vesci and G. Natile, *J. Med. Chem.*, 2005, **48**, 7821–7828.

26 J. J. Wilson and S. J. Lippard, *J. Med. Chem.*, 2012, **55**, 5326–5336.

27 E. Wexselblatt, R. Raveendran, S. Salameh, A. Friedman-Ezra, E. Yavin and D. Gibson, *Chem.–Eur. J.*, 2015, **21**, 3108–3114.

28 F. F. Liu, S. H. Gou, F. H. Chen, L. Fang and J. Zhao, *J. Med. Chem.*, 2015, **58**, 6368–6377.

29 X. C. Huang, R. Z. Huang, S. H. Gou, Z. M. Wang, Z. X. Liao and H. S. Wang, *Bioconjugate Chem.*, 2016, **27**, 2132–2148.

30 J. Pracharova, T. Saltarella, T. R. Radosova Muchova, S. Scintilla, V. Novohradsky, O. Novakova, F. P. Intini, C. Pacifico, G. Natile, P. Ilik, V. Brabec and J. Kasparkova, *J. Med. Chem.*, 2015, **58**, 847–859.

31 G. N. Kaluderović, S. A. Mijatović, B. B. Zmejkovski, M. Z. Bulatović, S. Gómez-Ruiz, M. K. Mojić, D. Steinborn, D. M. Miljković, H. Schmidt, S. D. Stošić-Grujičić, T. J. Saboe and D. D. Maksimović-Ivanić, *Metallomics*, 2012, **4**, 979–987.